SELF-MONITORING OF FREEZE-THAW DAMAGE USING TRIPHASIC ELECTRIC CONDUCTIVE CONCRETE

Yining DING[a*], Yesheng HUANG[a], Yulin ZHANG[b], Said JALALI[c], J.B. AGUIAR[c]

[a)]State Key Laboratory of Coastal and Offshore Engineering, Dalian University of Technology, Dalian 116023, China
[b)]Centre of Mathematics, University of Minho, Braga 4700-052, Portugal
[c)]Department of civil engineering, University of Minho, Braga, Portugal

*****Yining DING Tel:008641184709756; Email:ynding@hotmail.com*

Abstract

The effect of freeze-thaw cycles on concrete is of great importance for durability evaluation of concrete structures in cold regions. In this paper, damage accumulation was studied by following the fractional change of impedance (FCI) with number of freeze-thaw cycles (N). The nano-carbon black (NCB), carbon fiber (CF) and steel fiber (SF) were added to plain concrete to produce the triphasic electrical conductive (TEC) and ductile concrete. The effects of NCB, CF and SF on the compressive strength, flexural properties, electrical impedance were investigated. The concrete beams with different dosages of conductive materials were studied for FCI, N and mass loss (ML), the relationship between FCI and N of conductive concrete can be well defined by a first order exponential decay curve. It is noted that this nondestructive and sensitive real-time testing method is meaningful for evaluating of freeze-thaw damage in concrete.

Key words: Micro carbon fibers, Macro steel fibers, Nano carbon black, Conductive concrete, Fractional change in impedance, Freezing and thawing damage.

1. Introduction

With the deterioration of concrete structures, durability is of great concern. For structures in cold regions, freeze–thaw cycling is especially one of the main reasons of concrete damage. The degradation stems from the freezing of the water in concrete upon cooling, and the thawing upon subsequent warming. The phase transition causes dimensional change and internal stress change, and repeated cycles of freezing and thawing have a cumulative effect on the damage rather than a single occurrence of frost [1]. Previous investigation on the freeze–thaw durability of concrete has been focused on the property degradation of modulus and strength [2-3], weight loss and length change [2-5], microstructural change [6] and ultrasonic wavevelocity change [7] after different amounts of freeze–thaw cycling. However, these methods are usually used on laboratory specimens, and not very suitable for detecting the damage of concrete member in situ and in real-time.

Concrete with conductive materials is capable of sensing its own stress, strain and other damages like cracking by the electrical resistance measurement [8-16]. Furthermore, electrical conductive concrete (CC) can also provide wide prospect in specialist applications, such as vibration control,

electromagnetic shielding, traffic monitoring and deicing [13-14]. In this study, SF, CF and NCB were added into concrete as conductive phases for producing the triphasic electric conductive concrete, which allows to monitor the freeze–thaw damage by the FCI of itself without the need of embedded, attached or remote sensors.

On the one hand, the macro fibers as structural materials could mitigate the internal stress concentration in the concrete matrix caused by freezing and thawing cycles and increase the flexural toughness of concrete member before and after freezing and thawing cycles [6, 8]. On the other hand, as function materials, the well distributed SF and CF in the concrete matrix can form some continuous conductive pathways which carry current and play a fundamental role in the electrical transport process, consequently enhance electrical conductivity of concrete [11, 16]. The addition of NCB may improve the electrical conductivity, the toughness of the aggregate interface in the concrete matrix with lower cost. The combined application of NCB, micro CF and macro SF in concrete can enhance the conductivity of the concrete by using the conductive network of fibers and the electric characteristics of the NCB, and at the same time the mechanical property of the concrete can also be improved [11, 16-17]. The initiation and evolution of strain and damage in the concrete caused by the internal stress due to the freeze–thaw cycling can induce the change of conductive pathways [15, 16], which result in the change of impedance of concrete.

Wang [18] used the electrical resistivity methods to assess the micro structure alteration of cement-based materials by freeze-thaw action. They found electrical resistivity and temperature showed a bilinear relationship in logarithmic coordinates. Chung and Cao [9] investigated the damage evolution during freeze-thaw cycling of cement mortar involving damage accumulating gradually until failure. The results indicated that a temperature increment may cause the decreasing of resistivity reversibly, whereas damage causes the increasing of resistivity irreversibly, however, the experiments were performed on the cement mortar, and not on the concrete. Cai and Liu [19] studied the ice formation process in concrete pores by following the change of electrical conductivity of concrete, but just within one freeze-thaw cycle without consideration of damage. The investigation regarding the accumulation of concrete damage during freeze–thaw cycles using the FCI is still very rare.

In this paper, based on the investigation of the NCB, CF and SF on compression strength and flexural performance of concrete, a series triphasic conductive material reinforced concrete beams were experimentally studied, in order to analyze the damage and the FCI of beam under freeze-thaw cycles, especially to study the relationships between FCI and the damage degree of concrete under freeze-thaw cycles. The relationship between the FCI and the number of freeze–thaw cycles of concrete beam was established via the regression analysis, and this relationship can be well fitted by an Exponential Decay First Order curve.

2. Experimental Investigations

2.1 Materials and mixture

The base mix design of concrete samples without conductive admixture (NCB, CF and SF) was as follows: cement CEM I 42.5R 390 kg/m^3, fly ash 155 kg/m^3; The fine aggregate 848 kg/m^3 (0-5 mm) was Silica sand with 2.51 fineness modulus. The coarse aggregate 822 kg/m^3 (5-10 mm) was crushed limestone; water 272.5 kg/m^3; water binder ratio 0.5, Super-plasticizer (SP) 7.63 kg/m^3 (1.4% by mass of the binder).

The content of NCB with particle size ca. 30 nm – 90 nm (Fig. 1(a) and 1(b)) varies from 0.55 kg/m^3 up to 1.64 kg/m^3 for different mixtures (between 0.1% and 0.3% by mass of binder), the density of NCB was about 0.5 g/cm^3 and the volume resistivity was 0.35 Ω•cm. The CF content with diameter of 12-15 μm and length of 6 mm (Fig.1(c)) varies from 2.18 kg/m^3 up to 6.54 kg/m^3 for different mixtures (between 0.4% and 1.2% by mass of binder), the density of CF was about 1.6 g/cm^3 and the volume resistivity of CF was 1.6x10^{-3} Ω•cm; ca. 600 million pieces/kg. The macro SF content with diameter of 0.55 mm and length of 35 mm (Fig.1(d)) varies from 22 up to 44 kg/m^3 (between 4% and 8% by mass of binder), the density of SF was about 7.85 g/cm^3 and the volume resistivity of SF was 10^{-7} Ω•cm, ca. 15000 pieces/kg. A methylcellulose was used in the amount of 0.4% by mass of cement to dispose the CF and a Tributylphosphate as defoamer was used in the amount of 0.19% of sample volume. The base mix design of concrete without conductive materials is illustrated in Table1, and the basic mix design is used also for the investigated conductive concrete samples.

The different dosages of the conductive admixtures (NCB + CF + SF) by mass of binder in various concrete samples are compared and listed in Table 2. The serial numbers are fixed according to the different types and different contents of conductive phases. For instance, "T02084" represents the concrete sample added with NCB of 0.2%, CF of 0.8% and SF of 4% by mass of binder.

Table 1 Mix design of reference concrete

Cement (kg/m^3)	Fly ash (kg/m^3)	Fine aggregate (kg/m^3)	Coarse aggregate (kg/m^3)	Water (kg/m^3)	SP (kg/m^3)
390	155	848	822	272.5	7.63

Table 2 Comparison of the dosages of the conductive admixtures

Serial number	NCB		CF		SF		Total vol%
	mass/binder%	vol%	mass/binder%	vol%	mass/binder%	vol%	
PC	0	0	0	0	0	0	0
T02084	0.20(1.09kg/m^3)	0.27	0.80(4.36kg/m^3)	0.27	4.00(22kg/m^3)	0.28	0.82
T01124	0.10(0.55kg/m^3)	0.14	1.20(6.54kg/m^3)	0.41	4.00(22kg/m^3)	0.28	0.83
T01128	0.10(0.55kg/m^3)	0.14	1.20(6.54kg/m^3)	0.41	8.00(44kg/m^3)	0.56	1.11
T03048	0.30(1.64kg/m^3)	0.41	0.40(2.18kg/m^3)	0.14	8.00(44kg/m^3)	0.56	1.11

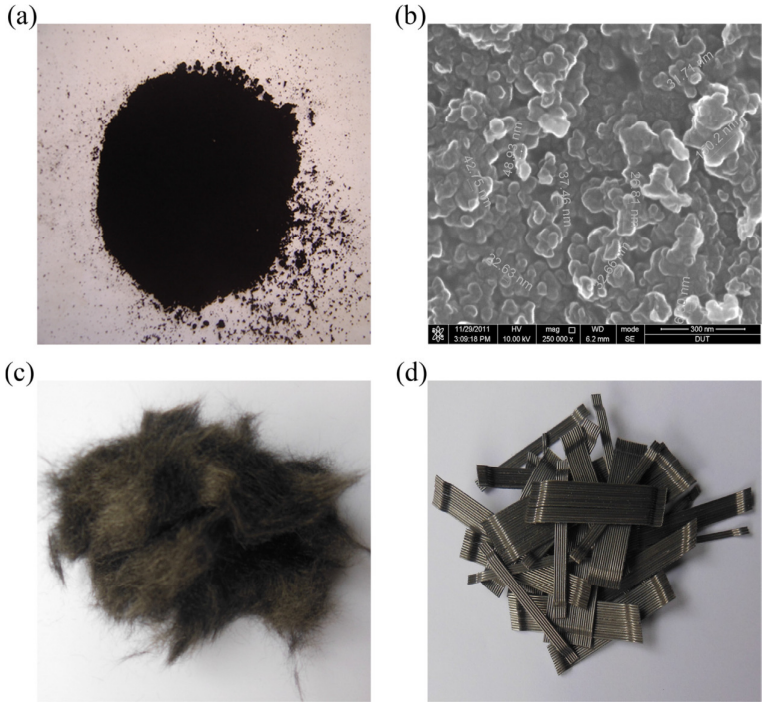

Fig. 1. (a) Nano carbon black, (b) Particle size of nano carbon black using High Resolution Field Emission SEM, (c) Carbon fiber and (d) Macro steel fiber

2.2 Samples and set-up description

A forced mixer was used for mixing. For concrete specimens with conductive admixtures, NCB was mixed firstly with cement, fine and coarse aggregate before adding of water, however, the CF, methylcellulose and defoamer were dissolved or pre-mixed with 5 liter water for well dispersion of fibers. Then the pre-mixture, NCB and superplasticizer, cement, fly ash and aggregate, water and SF were mixed 3 min. The specimen prepared for testing was beams with the size of 100 mm×100 mm×400 mm (Fig.2). After pouring the mix into molds, an external electric vibrator was used to facilitate compaction and decrease the amount of air bubbles. The specimens were demolded after 1 day and then cured at 23±3°C and 95-100% relative humidity for 28 days. Then four electrical contacts were prepared in the form of conductive adhesive tape, which was wrapped around the specimen. Based on the four probe method of electric resistance measurement, the outer two contacts A and D were for passing current while the inner two contacts B and C were for measuring of voltage [16-20]. The A.C. stabilized voltage supply with frequency of 50 Hz and a Digit multimeter (KEITHLEY 2100 6/12) were used to measure the voltage, the impedance has been calculated. For protection of the electrodes made with conductive tape during the fast freeze–thaw cycle, epoxy resin was coated to the electrode surface. The FCI measured is the fractional change in volume resistance of specimen. The dimensions and electrical contact details of all beams are shown in Fig. 2.

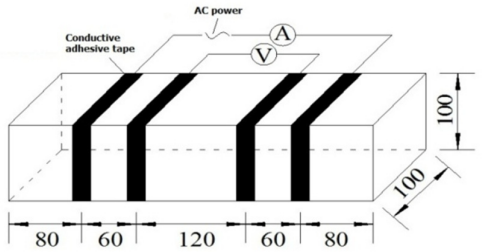

Fig.2 Specimen configuration for measuring impedance.

The supply voltage and frequency in this work were fixed in the value of 60 V and 50 Hz respectively [21]. As the fast freeze-thaw cycle was carried out in a immersion state, the specimens were immersed in water of 20±2°C for four days before freeze-thaw cycle testing, the impedance of beams before and after immersion was measured to identify the effect of the immersion. Then the concrete specimens were placed in a freezing and thawing machine which operates 8-9 cycles per day with a specimen core temperature ranging from -18°C to 5°C according to ASTM C 666 testing specifications [22]. Specimens were removed from the freeze-thaw machine each 10 cycles and 50 cycles for measuring the value of impedance and mass of concrete. Previous investigations indicated that the impedance varies largely with temperature in the freeze-thaw cycle [9, 18], so the specimens removed from the machine was placed in the curing room for 24 hours before measurement was taken.

The 100×100×100 mm cube specimens for compression strength were tested at the ages of 28 days. The 100×100×400 mm beams were tested under flexure on a span of 300 mm in four-point loading using a hydraulic servo testing machine (MTS 810). The flexural test is determined by the deformation-controlled experiment. A close loop test machine is used and the deflection is measured using two LVDTs, the deformation rate of the mid span is 0.2 mm/min until a specified deflection of 3.5 mm. The load–deflection curves are used to evaluate the flexural strength and flexural toughness of conductive concrete beams (Fig.4). The energy absorption of conductive concrete is determined in accordance with the following expression:

$$D_{BZ} = \int_0^{\delta_i} F(x)dx$$

3. Results and Discussion

3.1 Effect of conductive materials on the compressive strength

The average values of the compressive strength (f_{cu}) of three specimens at the age of 28 days are listed in Table 3. Compared with plain concrete (PC) without any conductive admixtures, the increment of the compression strength ranges between 2.5% and 7%. From Table 3 and previous studies [8, 15, 17, 24, 25], it can be seen that the addition of fibres and NCB with low contents aids in converting the brittle properties of concrete into a ductile material, but no significant trend of improving compressive strength was observed.

Table 3 Comparison of the compressive and flexural strength, the equivalent flexural strength and energy absorption of beams with different conductive admixtures

Serial number	f_{cu} MPa	F_u kN	σ_u MPa	D^f_{BZ2} kNmm	Equ.β_{BZ2} MPa	D^f_{BZ3} kNmm	Equ.β_{BZ3} MPa
PC	35.6	13.23	3.97	---	---	---	---
T02084	36.9	17.07	5.12	5.30	1.43	20.54	1.76
T01124	36.5	17.07	5.12	6.46	2.11	25.56	2.26
T01128	37.9	26.28	7.88	13.01	5.03	55.27	5.06
T03048	34.6	26.05	7.81	14.24	5.81	63.52	5.89

Where: F_u: maximum value of the load in the interval of 0.1 mm (kN); δ_1: deflection corresponds to the F_u (mm); D^b_{BZ}: energy absorption of the unbroken concrete (kN mm); $D^f_{BZ2} = D_{BZ2} - D^b_{BZ}$ (kN mm) by $\delta_2 = \delta_1 + 0.65$ (mm); $D^f_{BZ3} = D_{BZ3} - D^b_{BZ}$ (kN mm) by $\delta_3 = \delta_1 + 3.15$ (mm); Equ. β_{BZ2}: equivalent flexural tensile strength (MPa) by δ_2; Equ. β_{BZ3}: equivalent flexural tensile strength (MPa) by δ_3 [23 - 24].

3.2 Effect of conductive materials on the flexural behaviours

Fig. 4 illustrates the comparison of the load-deflection curves of plain concrete (PC) beam and beams with different NCB, CF and SF contents. Both the experiment and the calculation of the flexural strength and toughness parameters (the equivalent flexural strength/Equ.β_{BZ} and energy absorption capacity/D^f_{BZ}) are carried out based on the German Guideline [23]. The investigations of the SF and hybrid fiber effect on the bending behavior (strength and toughness parameters) of concrete are performed in [24]. The flexural strength (σ_u) and toughness parameters can be found in Table 3. From Table 3 and Fig.4, it can be seen that:

- Plain concrete (PC) beam showed clear brittle behavior and broken down without any post crack energy absorption after cracking.
- Compared to PC without any conductive phases, two phenomena as follows can be observed: i) σ_u of conductive concrete (T01128, T03048) with 44 kg/m^3 SF and CF of 2.18 and 6.54 kg/m^3 at the elastic stage increased by 98% and 97%, respectively; ii) σ_u of T02084, T01124 with 22 kg/m^3 SF and CF of 4.36 and 6.54 kg/m^3 increased by 29%.
- The reason of the strong increasing of σ_u can be traced back to the following three points: a) The addition of micro CF could enhance the σ_u of concrete due mainly to the huge amount of fiber pieces (ca. 600 million pieces/kg) which may form a dense fiber net in the concrete matrix (Each beam contains 5 million up to 15 million pieces of micro CF and 1300 up to 2600 pieces of macro SF) and increase the first crack strength clearly. b) The increasing of σ_u can be caused by the positive hybrid effect as well as the interlocking between micro CF and macro SF. c) Other investigations of Baeza and Deng [29 – 31] confirmed also that the flexural strength of concrete increased with the increasing of CF content and hybrid fiber content clearly, compared to plain concrete.
- Compared to post-crack behavior of beams with 22 kg/m^3 SF (T01124, T02084), the triphasic conductive beams with 44 kg/m^3 SF (T01128, T03048) behave much better over the entire deflection range. The hybrid use of NCB, micro CF and macro SF has positive hybrid effect on the flexural toughness, and the SF plays a dominant role in improving the flexural behavior, especially in flexural toughness. For instance, the energy absorption Equ.β_{BZ3} of T01128

increased about 120% compared to that of T0124, whereas the macro SF content increased only 100%.

These observations supports the use of fibre cocktail in conductive ductile concrete because the huge amount of micro carbon fibre can better prevent the further pulling out of the macro steel fibres from the concrete matrix after the cracking [24, 26, 29 - 31].

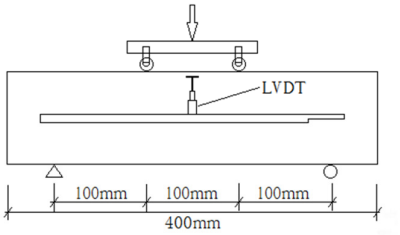

Fig.3 Four-point bending test set-up and arrangement of displacement sensors

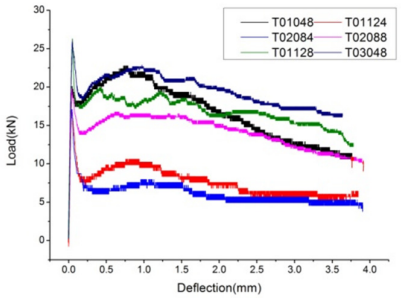

Fig.4 Comparison of load-deflection curves of conductive concrete beams

4. Impedance of concrete beam before and after immersion

The influence of conductive admixtures on the impedance value of concrete beam before immersion ($|Z_0|$) and after immersion ($|Z'_0|$) before freeze-thaw cycle testing are listed in Table 4.

Table 4 Results of initial impedance of conductive concrete beams before freeze-thaw cycle testing

Serial number	Total vol%	$\|Z_0\|(\Omega)$	$\|Z_0'\|(\Omega)$	Variation(%)
PC	0	8000	7419.35	-7.25
T02084	0.82	2018.93	1190.16	-41.03
T01124	0.83	1792.14	1296	-27.68
T01128	1.11	1319.05	1084.94	-17.81
T03048	1.11	1339.13	973.42	-27.3

From Table 4 it can be observed that:

- The impedance $|Z_0|$ and $|Z_0'|$ decreased clearly by addition of conductive materials (NCB, CF and macro SF), especially by addition of SF. Compared with PC beam without any conductive

admixtures, the impedance $|Z_0|$ of triphasic conductive concrete decreased between 75% (beams with 22 kg/m^3 SF) and 85% (beams with 44 kg/m^3 SF) with the increasing of content of conductive materials; The impedance $|Z_0'|$ of triphasic conductive concrete decreased about 85%.

- Also the impedance ($|Z_0|$) reduced strongly after four days immersion and the triphasic conductive concrete showed a larger reduction in impedance than that of PC samples. The impedance $|Z_0|$ of triphasic conductive concrete decreased between 17.8% and 41.03%, while $|Z_0|$ of PC decreased only 7.25% after four days immersion.

4.1 Fractional change of impedance, numbers of freeze-thaw cycles and mass loss

The variation in the impedance expressed in terms of FCI can be expressed in Eqn. (1):

$$FCI_i = \frac{|Z_i| - |Z'_0|}{|Z'_0|} \times 100\% \quad (1)$$

Where $|Z_0'|$ is defined as the initial impedance value before freeze-thaw cycles, and $|Z_i|$ is the impedance value after *i* freeze-thaw cycles.

In order to verify the validity of FCI to estimate the frost resistance of triphasic conductive concrete, the ML [27 – 28] and the impedance value were recorded every 10 freeze-thaw cycles if N was less than 100; and they were measured every 50 freeze-thaw cycles if N was higher than 100. The ML was tested carried out according to China National Guideline and Japan Industrial Standard [27 - 28] and can be evaluated according to Eqn.(2). The results of FCI and ML up to 300 freeze-thaw cycles are listed in Table 5.

$$\text{Mass loss} = (m - m_i) / m \quad (2)$$

Where m: the initial mass before freeze - thaw cycles; m_i: the mass after i freeze - thawing cycles

Table 5 FCI and ML of fast freeze-thaw cycles tests

Freeze -thaw cycles	T 02084		T 01124		T 01128		T 03048		PC
	ML (%)	FCI (%)	ML (%)	FCI (%)	ML (%)	FCI (%)	ML (%)	FCI (%)	ML (%)
0	0	0	0	0	0	0	0	0	0
10	0.043	-9.35	0	-0.99	0.042	-2.53	0.033	-1.79	0.032
20	0.097	-11.51	0.076	-1.89	0.148	-4.08	0.033	-3.06	0.032
30	0.097	-19.00	0.197	-9.15	0.148	-14.09	0.197	-16.32	0.075
40	0.152	-20.73	0.251	-12.69	0.200	-17.77	0.230	-17.94	0.096
50	0.206	-21.16	0.284	-12.79	0.232	-18.34	0.252	-19.46	0.139
60	0.260	-22.26	0.361	-14.36	0.306	-21.02	0.274	-20.54	0.171
70	0.282	-27.15	0.459	-16.07	0.506	-24.37	0.329	-21.98	0.299
80	0.412	-29.49	0.481	-17.67	0.527	-29.35	0.329	-24.07	0.502
90	0.499	-31.77	0.557	-23.03	0.538	-31.62	0.559	-28.36	0.513
100	0.597	-34.51	0.568	-22.02	0.569	-32.31	0.746	-32.29	0.641
150	0.707	-36.82	0.772	-34.51	0.711	-46.91	0.955	-40.76	0.962
200	1.312	-40.17	1.312	-42.69	1.088	-51.85	1.445	-42.26	1.126
250	1.345	-41.97	1.409	-46.68	1.278	-61.83	1.523	-49.95	1.171
300	1.758	-42.86	1.578	-49.66	1.582	-63.28	1.715	-51.42	1.424

From Table 5, it can be observed that: the value of FCI was negative, which means the impedance of triphasic conductive concrete declined with the increased freeze-thaw cycles; however, the absolute value of FCI (|FCI|) increased with the increased freeze-thaw cycles, which was consistent with the increased ML [27], an indicator widely used to estimate frost resistance of concrete materials.

Fig.5 demonstrated the comparison of relationships of numbers of freeze-thaw cycles (N) and ML between plain concrete and some conductive concretes. From Fig.5 and Table 5, it can be seen that the ML of plain concrete and conductive concrete increased with the increasing of Freeze - thaw cycles, and the increasing trend of ML of plain concrete is consistent with that of triphasic conductive concrete. There is a linear relationship between ML and N for both PC and conductive concrete with very high Pearson coefficient between 0.96 and 0.99. Furthermore, the slopes of all conductive concrete are higher than that of PC, which means that the conductive concrete will reach the limit value of ML (i.e. freeze thaw resistance) prior to plain concrete. Hence, the ML of conductive concrete may reflect ML of plain concrete safely. In addition, among the conductive concrete, T03048 (with the highest NCB content of 1.64 kg/m^3) shows the highest slope, and T01128 (with the lowest NCB content of 0.55 kg/m^3) shows the lowest slope.

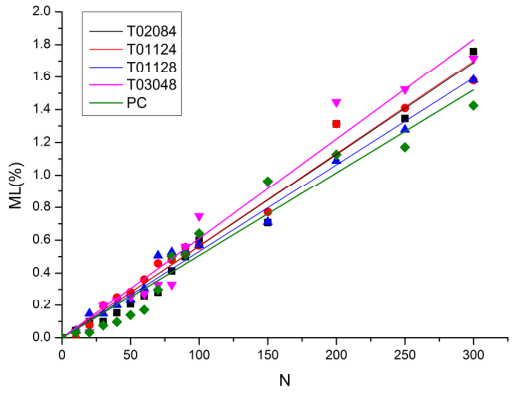

Fig.5 Comparison of mass loss (ML) - cycles number (N) relationships between PC and conductive concretes

4.2 Relationship between the number of freeze–thaw cycles (N) and FCI of electric conductive concrete beams

Fig. 6 illustrates the relationship between the number of freeze–thaw cycles (N) and the FCI of conductive concrete beams. It can be seen that this relationship corresponds well with the function of first order exponential decay, which can be expressed in Eqn. (3):

$$FCI = a\exp(-N/b) + c \tag{3}$$

Where: a, b and c are constant parameters corresponding to the types and the contents of electric conductive phases, a/b is the slope of the curves in Fig.6 where N=0; c means the asymptote of the curves; the variable N is number of freeze–thaw cycles.

The parameters fitted and the correlation coefficient (R^2) of all electric conductive concrete beams with different types and contents of conductive phases are listed in Table 6. The correlation coefficients of all conductive concrete beams vary between 0.93656 and 0.98841.

Table 6 Fitted parameters of regression equation of FCI - N

Serial number	a	b	c	FCI after 300 cycles (%)	R^2
T02084	40.87	71.68	-42.96	-42.86	0.9822
T01124	72.25	230.56	-70.25	-49.66	0.9871
T01128	84.27	190.07	-83.44	-63.28	0.99355
T03048	55.53	117.88	-54.54	-51.42	0.9722

From Fig. 6 and Table 6, it can be seen that:

(1) The curves in Fig. 6 demonstrate a monotone decreasing relationship between FCI and N. The absolute value of FCI of conductive concrete beams increases with the increasing of the number of freeze–thaw cycles.

(2) The R^2 of beams with conductive phases is higher than 0.97. Hence, the relationship between FCI and the number of freeze–thaw cycles is quite strong correlated with Eqn. (3).

(3) The R^2 of T01128 beam is higher than 0.99. It means that the relationship between FCI and the number of freeze–thaw cycles is very strong correlated with the Eqn. (2), and the self-sensing of the freeze–thaw damage could be more suitable especially for concrete members with above suggested types and contents of conductive admixture.

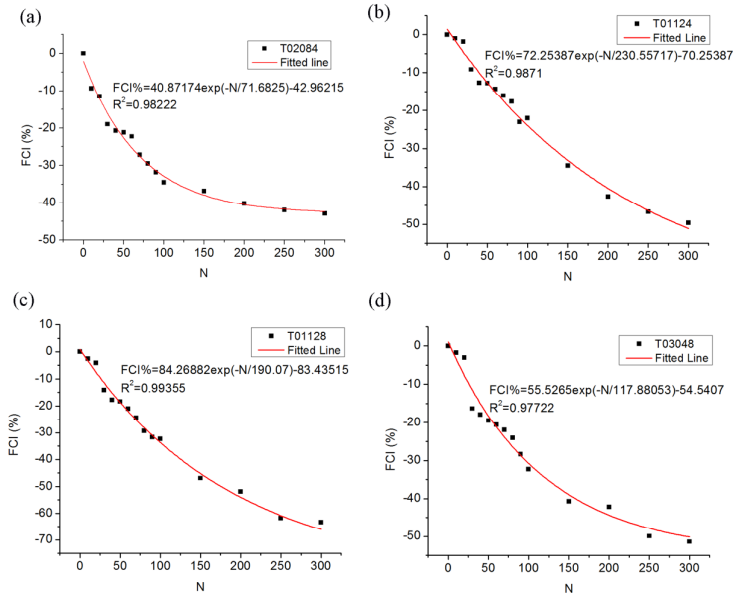

Fig.6 Relationship between the fractional change of impedance (FCI) and the number of freeze–thaw cycles (N) of (a)T02084, (b)T01124, (c)T01128 and (d)T03048

5. Conclusion

The purpose of this study is to explore the application of the NCB, CF and SF as triphasic electric conductive materials for self-sensing of the freeze–thaw damage of concrete beam. A series of investigations on the electric properties like the impedance value and the relationship between FCI-N have been carried out. The effects of conductive materials on the compressive strength, flexural performance and impedance value are also studied together with the change of ML when the freeze–thaw cycles are increased. The results of the investigation can be summarized as follows:

(1) The addition of NCB, CF and macro SF has a significant positive effect on both the flexural strength and toughness. The macro SF plays a dominant role in improving the flexural strength and toughness.

(2) The impedance $|Z_0|$ and $|Z_0'|$ decreased visibly with the addition of NCB, CF and especially by addition of SF. Compared to plain concrete the decrease in impedance $|Z_0|$ of conductive concrete was more noticeable after immersion.

(3) The ML of conductive concrete can reflect that of plain concrete, and the conductive concrete will reach the maximum value of mass loss prior to plain concrete.

(4) It is interesting to note that the relationship between FCI and number of freeze–thaw cycles (N) corresponds well with the Exponential Decay First Order curve with high correlation coefficients between 0.977 and 0.994. This self - monitoring ability of conductive concrete is a nondestructive tool for assessing the concrete damage under freeze-thaw cycles.

Acknowledgement

The authors acknowledge the National Natural Science Foundation of China (Grant: 51578109) and (Grant: 51121005), and Fundação para a Ciência e a Tecnologia (SFRH/BPD/22680/2005), the FEDER Funds through “Programa Operacional Factores de Competitividade - COMPETE" and by Portuguese Funds through FCT - within the Projects PEst-CMAT/UI0013/2011, PTDC/MAT/112273/2009.

References

[1] Neville A, Brooks J. Concrete Technology. Addison Wesley Longman Limited, London, UK, 1999.

[2] Marzouk H, Jiang K. Effects of freezing and thawing on the tension properties of high -strength concrete. ACI Mater J, 1994; 91 (6): 577 – 586.

[3] Rutherford J, Langan BW, Ward MA. Use of control specimens in freezing and thawing testing of concrete. Cem Concr Aggreg, 1994; 16(1): 78 – 82.

[4] Bordeleau D, Pigeon M, Banthia N. Comparative study of latex-modified concretes and normal concretes subjected to freezing and thawing in the presence of a deicer salt solution, ACI Mater J, 1992; 89(6): 547 – 553.

[5] Sabir B. Mechanical properties and frost resistance of silica fume concrete. Cem Concr Compos, 1997; 19 (4): 285 – 294.

[6] Yun H. Effect of accelerated freeze-thaw cycling on mechanical properties of hybrid PVA and PE fiber-reinforced strain-hardening cement-based composites (SHCCs). Compos PART B-ENG, 2013; 52:11-20.
[7] RILEM TC 176 – IDC 2002: Recommendations of RILEM TC 176: Test methods of frost resistance of concrete.
[8] Ma X. Study on crack and freeze-thaw resistance of hybrid fibers reinforced high performance concrete. Master dissertation, Dalian University of Technology; 2006 [in Chinese].
[9] Cao J, Chung D. Damage evolution during freeze–thaw cycling of cement mortar, studied by electrical resistivity measurement. Cem Concr Res, 2002; 32:1657–1661.
[10] Wang S, Chung D. Self-sensing of flexural strain and damage in carbon fiber polymer-matrix composite by electrical resistance measurement. Carbon, 2006; 44:2739–2751.
[11] Li H, Xiao H, Ou J. Effect of compressive strain on electrical resistivity of carbon black-filled cement-based composites. Cem Concr Compos, 2006; 28 : 824–828.
[12] Vaidya S, Allouche E. Strain sensing of carbon fiber reinforced geopolymer concrete. Mater Struct, 2011; 44:1467–1475.
[13] Chung D. Carbon materials for structural self-sensing, electromagnetic shielding and thermal interfacing. Carbon, 2012; 50(9): 3342-3353.
[14] Sanchez F, Sobolev K. Nanotechnology in concrete – A review. Constr Build Mater, 2010; 24: 2060–2071.
[15] Ding Y, Chen Z, Han Z, Zhang Y, Pacheco-Torgal F. Nano carbon black and carbon fiber as conductive materials for the diagnosing of the damage of concrete beam. Constr Build Mater, 2013; 43:233–241.
[16] Ding Y, Han Z, Zhang Y, Azevedo C. Hybrid Use of Steel and Carbon Fiber Reinforced Concrete for Monitoring of Crack Behaviour. ECCM15 - 15TH European Conference on Composite Materials, Venice, Italy, 24-28 June 2012.
[17] Wen S, Chung D. Partial replacement of carbon fiber by carbon black in multifunctional cement-matrix composites. Carbon, 2007; 45:505–513.
[18] Wang Z, Zeng Q, Wang L. Characterizing blended cement pastes under cyclic freeze–thaw actions by electrical resistivity. Constr Build Mater, 2013; 44: 477-486.
[19] Cai H, Liu X. Freeze–thaw durability of concrete: ice formation process in pores. Cem Concr Res, 1998; 28 (9): 1281 – 1287.
[20] Tian X, Hu H. Test and Study on Electrical Property of Conductive Concrete. Procedia Earth and Planetary Science, 2012; 5: 83 – 87.
[21] Reza F, Batson G, Yamamuro J, Lee J. Volume electrical resistivity of carbon fiber cement composites. ACI Mater J, 2001; 98(1): 25-35.
[22] ASTM Standard Test Method for Resistance of Concrete to Rapid Freezing and Thawing. C666/C666M-03(2008)
[23] Deutscher Beton-Verein EV, DBV-Merkblatt. Bemessungsgrundlagen fuer Stahlfaserbeton im Tunnelbau, Wiesbaden: Eigenverlag; 1998.
[24] Ding Y, Zhang Y, Thomas A. The investigation on strength and flexural toughness of fibre cocktail reinforced self-compacting high performance concrete. Constr Build Mater, 2009; 23: 448-452.
[25] Ding Y. and Kusterle W.: Compressive Stress-Strain-Relationship of Steel Fibre Reinforced Concrete at Early Age, Cement and Concrete Research, 2000; 30(10); 1573-1579.
[26] RILEM TC 162-TD: Test and design methods for steel fibre reinforced concrete, Materials and

Structures/Matériaux et Constructions, 2000; 33, 3-5.
[27] China National Guideline, Standard for test methods of long-term performance and durability of ordinary concrete, GB/T 50082-2009.
[28] Japan Industrial Standard, Method of test for resistance of concrete to
freezing and thawing", 2010, JIS A 6204-2000.
[29] Baeza, F.J. et al: Effect of aspect ratio on strain sensing capacity of carbon fiber reinforced cement composites, Materials and Design, 2013; 51: 1085 – 1094.
[30] Ferrari V. J. et al: Flexural strengthening of reinforcement concrete beams using high performance fiber reinforcement cement-based composite (HPFRCC) and carbon fiber reinforced polymers (CFRP), Construction and Building Materials, 2013; 48: 485 – 498.
[31] Deng Z.: The fracture and fatigue performance in flexure of carbon fiber reinforced concrete, Cement & Concrete Composites, 2005; 27: 131 – 140.